# Assessment of Vertically Integrated Liquid (VIL) Water Content Radar Measurement

BRICE BOUDEVILLAIN AND HERVÉ ANDRIEU

*Division Eau, Laboratoire Central des Ponts-et-Chaussées, Nantes, France*

(Manuscript received 15 June 2002, in final form 30 October 2002)

ABSTRACT

Vertically integrated liquid (VIL) water content is a parameter obtained from a radar performing voluminal scanning. This parameter has proven useful in the detection of severe storms and may be a worthwhile indicator for very short-term rainfall forecasting methods. Unfortunately, no information is available on the accuracy of VIL radar measurements. The present paper addresses this issue by means of simulation. Reference VILs are defined from vertical profiles of drop size distributions (DSD). These profiles make it possible to simulate the corresponding vertical profiles of reflectivity as well as the radar measurements used to deduce the VIL, as estimated classically (i.e., application of a classical relationship between equivalent radar reflectivity factor $Z_e$ and liquid water content $M$ adapted to raindrops). A comparison of the reference VIL to the corresponding estimate then allows estimating radar measurement error. The VIL measurement error is first studied from two hypothetical, yet realistic, vertical profiles of DSD: one typical of stratiform rain and the other typical of a convective situation. A sensitivity analysis with respect to both meteorological conditions and radar operating conditions is also performed on these two profiles. For the convective case, use of a classical $Z_e$–$M$ relationship adapted to liquid water results in a significant underestimation of the reference VIL value. The same effect applies to the stratiform profile, even though brightband phenomena can compensate for this underestimation and lend the impression of smaller measurement error. A simple alternative method is proposed in order to reduce measurement errors. Both conventional and alternative VIL measurement methods are tested on the two theoretical profiles as well as on a series of actual vertical profiles of reflectivity. Better measurements are obtained with the alternative method, provided the altitude of the 0°C isotherm and the density of ice particles can be determined with reasonable precision. This alternative method for estimating VIL from radar data could serve to improve VIL measurement accuracy and would be worth applying to a longer series of observed data.

## 1. Introduction

Real-time surveys of rainfall fields and measurement of rainfall rates have for a long time constituted the primary objective of operational weather radar networks. The deployment of modern radar networks has allowed for more refined atmospheric sampling by providing additional radar information: voluminal scanning, Doppler velocity, etc. As illustrated by the Next Generation Radar (NEXRAD; Klazura and Imy 1993) or in Europe (European Commission 2001), new radar data products have been made available to users. Research has been undertaken to take advantage of these new products. The vertically integrated liquid water content (hereafter denoted VIL) constitutes one such product. VIL actually represents the atmospheric water content that can be measured by classical (C or S band) weather radars and stands for the precipitation water content. Investigations conducted on the use of VIL have mainly been oriented in two directions: hail and severe storm warning, and quantitative rainfall forecasting.

Amburn and Wolf (1997) indicated that the probability of a thunderstorm producing hail at ground level increases once VIL density exceeds a threshold of 3.5 g m$^{-3}$. Billet et al. (1997) proposed a logistic regression algorithm based on both meteorological parameters and VIL to predict the probability of hail size exceeding 1.9 cm. Kitzmiller et al. (1995) observed that VIL acts as a discriminator between severe and non-severe thunderstorms. Shafer et al. (2000), in studying a storm system, observed that the cloud-to-ground flash density and other variables, such as reflectivity and VIL, evolve similarly. The efficiency of VIL-based algorithms for hail detection is a topic regularly addressed at radar conferences and does not yet appear to be fully established, as results obtained by Edwards and Thomson (1998) have confirmed.

Following the work of Georgakakos and Bras (1984), Seo and Smith (1992) and then French and Krajewski (1994) introduced VIL into very short-term rainfall forecasting models. The basic idea therein consists of a simple, yet physically based, model of the evolution of the VIL contained in atmospheric columns that move in

*Corresponding author address:* Brice Boudevillain, Division Eau, Laboratoire Central des Ponts-et-Chaussées, BP 4129, F 44341 Bouguenais Cedex, France.
E-mail: Brice.boudevillain@lcpc.fr

accordance with the rainfield velocity. Such an approach seeks to add a dynamic component to very short-term rainfall forecasting techniques that utilize the advection of rainfields. This model has been adapted and tested within an orographic context (Andrieu et al. 1996). Although encouraging, the results obtained were not fully decisive, partly because of the poor quality of the radar data used. Nevertheless, the potential utility of VIL for very short-term rainfall forecasting models has been confirmed in a number of ways: (i) simulation methods (Thielen et al. 2000; Dolcine et al. 2000), which take outputs from a mesoscale model as the reference values; and (ii) data analyses (MacKeen et al. 1997), which acknowledge that the sign of VIL evolution is related to the remaining storm lifespan. VIL has also been used in more detailed rainfall forecasting models. Lee and Georgakakos (1990, 1996) developed a rainfall simulation model that considers VIL measurement as the observation variable of a Kalman filter serving to adjust the instability index of the rainfall simulation model variable. Nakakita et al. (1996) and Sugimoto et al. (2000) determined the water vapor conversion rate of a physically based rainfall simulation model from VIL radar measurements. Ducrocq et al. (2000) pointed out that rainwater content estimated by radar was useful in initializing a finescaled model for convective system prediction.

Despite this rise in interest, very few studies have yet to focus on VIL measurement, which can only be performed by means of radar. French et al. (1995) addressed the influence of errors in reflectivity measurements. Klazura and Imy (1993) indicated that VIL ''reflectivity data converted into liquid water equivalent via an empirically derived relationship that assumes all reflectivity returns are from liquid water.'' Various parameters are liable to affect the accuracy of VIL measurements: variations in drop size distribution (DSD) characteristics, influence of the melting layer, presence of ice water in the upper part, and radar operating conditions (e.g., distance and beamwidth). The objective of this study is to quantify the influence of these parameters in order to assess the accuracy of VIL radar measurement. The adopted approach will be presented in the next section.

## 2. The adopted approach

The adopted approach consists of defining a reference VIL and then comparing it to the corresponding value measured by radar while performing voluminal scanning; this approach is based on simulation. The reliance upon simulation has been dictated for two reasons: it is not possible to measure VIL directly, and no comparison can be drawn between VIL measured indirectly by means of radar and a reference measurement. The variables used to characterize rainfall (i.e., intensity, rainwater content, and radar reflectivity) are bulk integrals of the DSD (Sempere-Torres et al. 1994). Consequently, the basis of the modeling approach lies in the definition

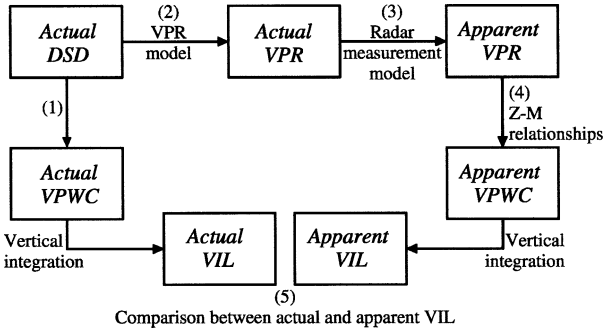


FIG. 1. Diagram of the approach adopted to estimate radar-based VIL measurement errors.

of DSD, which varies with altitude according to various factors that each represent a source of error in measuring VIL by radar. The adopted approach therefore encompasses the following steps (summarized in Fig. 1).

- Step 1: Choice of a vertical profile of DSD and meteorological conditions to allow both separating liquid from ice water and locating the melting layer. The vertical profile of DSD is transformed into a vertical profile of water content (VPWC) which, once integrated, provides the reference VIL.
- Step 2: Development of a model that enables transforming the vertical profile of DSD into a vertical profile of equivalent radar reflectivity factor (hereafter denoted VPR). This step accounts for meteorological information as well as the nature and types of hydrometeors that define the backscattering properties.
- Step 3: Simulation of the apparent VPR, that is, the VPR seen by a radar performing voluminal scanning; this step serves to introduce radar operating conditions.
- Step 4: Transformation of the apparent VPR into an apparent vertical profile of water content, from which the radar-measured VIL is deduced. The ''classical method'' for estimating rainwater content from radar reflectivity is based on a $Z_e$–$M$ relationship [see Eq. (22), section 4]; it will be compared with a slightly different approach, the ''alternative method,'' in the aim to improve the accuracy of VIL measurement.
- Step 5: Assessment of the radar-measured VIL.

The paper has been organized as follows. Section 3 describes the model for deriving the vertical profile of reflectivity from the vertical profile of DSD and summarizes the procedure used to simulate VIL radar measurement from the VPR. Section 4 discusses the influence of various errors on the VIL radar measurement, while section 5 presents the ''alternative'' VIL measurement method capable of mitigating the influence of these error sources. Section 6 is devoted to evaluating and comparing the classical and alternative methods; this assessment is based on actual data. The paper closes with a concluding section.

## 3. Modeling of vertical profiles of reflectivity and precipitation content

### *a. Development assumptions*

The vertical change in precipitation is driven by microphysical processes, described in detail by Pruppacher and Klett (1978) or by Rogers and Yau (1989). Microphysical processes are themselves controlled by the meteorological environment: temperature, pressure, and moisture. These processes result in vertical variations of the distribution of precipitation particles as they melt below the freezing level as well as in eventual changes to the size distribution of solid particles and particle density above the freezing level. An explicit model of microphysical processes would provide a detailed representation of the dynamics of precipitation formation and evolution, that is, the vertical changes in DSD features. Nevertheless, such a model would need to be coupled with a meteorological model; this combination would constitute a rather complex tool that involves many parameters and variables. This explicit modeling approach does not appear well-suited to studying the various sources of errors liable to affect VIL radar measurements. In order to achieve our goal, we have adopted a simplified model that does not include a representation of the microphysical processes; the vertical changes in DSD constitute the model inputs. The model developed allows focusing on the most influential parameters in VIL radar measurement and relies on the following assumptions.

- The reference variable is the DSD, which serves to generate all bulk variables defining precipitation characteristics: water content, radar reflectivity (Sempere-Torres et al. 1994), etc. The precipitation DSD conforms to an exponential distribution (Marshall and Palmer 1948):

$$N(D, h) = N_0 e^{-\Lambda(h)D}, \tag{1}$$

  where $N(D, h)$ ($m^{-4}$) is the number of drops with diameters between $D$ and $D + dD$ (m) per unit diameter range per unit air volume at altitude $h$ (m), $N_0$ ($m^{-4}$) is a measure of the total number of drops within the same unit volume, and $\Lambda(h)$ ($m^{-1}$) is the inverse value of the mean drop diameter at altitude $h$.
- Three types of water particles are distinguished: liquid, solid, and melting (hereafter denoted by the subscripts $l$, $s$, and $m$, respectively). For liquid particles, parameter $N_0$ of the DSD is assumed independent of altitude, which means that vertical DSD variations give rise to changes in $\Lambda$. This hypothesis is strengthened by the fact that $N_0$ is often assumed to be constant (Delrieu et al. 1991). It has been accepted that this assumption remains valid for solid particles as well.
- The melting layer is a narrow transitional zone in which the parameters influencing the backscattering properties of precipitation particles (mass density, dielectric constant, DSD) change very rapidly. The melting layer is capable of considerably enhancing the measured reflectivity (in the presence of the bright band). The melting process representation has already been addressed by several authors, with varying levels of description of the microphysical and thermodynamic processes (Willis and Heymsfield 1989; Klaassen 1988; Szyrmer and Zawadski 1999). The model used herein has been inspired from both Hardaker et al. (1995), which does not, however, take explicit account of thermodynamics, and Borga et al. (1997). In particular, the continuity of DSD at the solid/melting and melting/liquid transitions is ensured by assuming a one-to-one correspondence between solid particles and liquid raindrops.

### *b. Radar reflectivity and precipitation water content*

The general expression of precipitation content $M$ at altitude $h$ is given by

$$M(h) = \frac{\pi}{6} \int_{D_{\min}}^{D_{\max}} \rho(h) N(D, h) D^3 \, dD, \tag{2}$$

where $\rho(h)$ (kg $m^{-3}$) is the density of precipitation particles at altitude $h$, and $D_{\min}$ and $D_{\max}$ (m) the minimum and maximum diameters, respectively. It is usually accepted that: $D_{\min} = 0$ and $D_{\max} = \infty$ (Atlas et al. 1973).

Substituting $D_{\min}$ and $D_{\max}$ in Eq. (2) leads to the expression of VIL:

$$\text{VIL} = \int_0^{h_t} M(h) \, dh$$

with

$$M(h) = \frac{\pi \rho(h) N_0}{\Lambda^4(h)}, \tag{3}$$

where $h_t$ is the height at the top of the cloud.

Equivalent radar reflectivity factor at altitude $h$ can be expressed as follows:

$$Z_e(h) = \frac{\lambda^4}{\pi^5 |K(h)|^2} \int_0^{\infty} \sigma[D, \lambda, m(h)] N(D, h) \, dD, \tag{4}$$

with

$$|K(h)|^2 = \left| \frac{m^2(h) - 1}{m^2(h) + 2} \right|^2 \quad \text{and} \tag{5}$$

$$\sigma[D, \lambda, m(h)] = \frac{\lambda^2}{4\pi} \varphi[D, \lambda, m(h)], \tag{6}$$

with

$$\varphi[D, \lambda, m(h)] = \sum_{n=1}^{\infty} |(-1)^n (2n + 1)(a_n - b_n)|^2, \tag{7}$$

where $Z_e$ ($mm^6$ $m^{-3}$) is the equivalent radar reflectivity factor, $\lambda$ (m) the radar wavelength, $\sigma$ ($m^2$) the backscattering section of a water particle of diameter $D$, $K(h)$

the dielectric factor of precipitation particles, $m(h)$ the complex refractive index, and $a_n$ and $b_n$ the Mie coefficients dependent upon the complex refractive index and upon $\pi D/\lambda$ (Battan 1973).

Replacing $\sigma$ in Eq. (4) with the expression in Eq. (6) yields the final expression of equivalent radar reflectivity factor:

$$Z_e(h) = \frac{N_0\lambda^6}{4\pi^6|K(h)|^2}\int_0^\infty \varphi[D, \lambda, m(h)]e^{-\Lambda(h)D}\,dD. \quad (8)$$

Equations (3) and (8) confirm that equivalent radar reflectivity factor and precipitation water content expressions involve three variables that all depend on altitude: (i) the mean DSD diameter, (ii) the mass density of precipitation particles, and (iii) the complex refractive index of the particle. The next paragraphs describe the modelling of the vertical profiles of these variables which develop in three different layers: the lowest layer (hereafter referred to as the liquid layer), in which precipitation particles take the form of raindrops; the upper layer that contains ice water (hereafter the solid layer); and an inbetween melting layer that displays specific features.

### c. Vertical profile of precipitation particle mass density

In the lowest part of the atmosphere, precipitation particles are raindrops. Consequently, their mass density is constant and equal to

$$\rho(h) = \rho_l$$

with

$$\rho_l = 1000 \text{ kg m}^{-3}. \quad (9)$$

Above the 0°C isotherm, precipitation particles are ice particles and their mass density varies according to the type of hydrometeors: snowflakes, graupels, etc. In the following discussion, the mass density of solid particles will depend on the empirical density factor introduced by Klaassen (1988) and expressed as

$$\rho(h) = \rho_s = \rho_{s,\min}^{1-e}\rho_{s,\max}^{e}, \quad (10)$$

with $\rho_{s,\min} = 5$ kg m$^{-3}$ and $\rho_{s,\max} = 900$ kg m$^{-3}$, where $\rho_s$ is the mass density and $e$ the density factor that varies between 0 and 1 in order to cover the entire range of mass density. It is assumed herein that the density factor remains constant throughout the solid layer.

In the melting layer, precipitation particles are composed of a mixture of liquid and solid water, characterized by the melted mass fraction (defined as the melted mass divided by total particle mass). The melted mass fraction is approximated by a sine function, as suggested by Russchenberg (1992):

$$f_m(h) = \frac{1}{2}\left[\sin\left(\pi\frac{h_{\text{iso}0} - h}{h_{\text{iso}0} - h_{\min}} - 0.5\pi\right) + 1\right], \quad (11)$$

where $f_m(h)$ is the melted mass fraction, and $h_{\min}$ and $h_{\text{iso}0}$ denote the lowest latitude of the melting layer and the 0°C isotherm, respectively. The term $f_m$ increases from 0 at the solid layer boundary to 1 when reaching the liquid layer boundary.

The mass density of melting particles changes according to the melted fraction and is expressed by Borga et al. (1997) as

$$\rho(h) = \frac{\rho_l \times \rho_s}{\rho_l - f_m(h) \times (\rho_l - \rho_s)}. \quad (12)$$

### d. Vertical profile of the complex refractive index

The complex refractive index depends on radar wavelength, temperature, and the phase state of the scatterers.

In the liquid layer, it is typically accepted that the variation in refractive index with respect to wavelength and temperature is negligible, thereby leading to a dielectric constant of $|K(h)|^2 = 0.93$.

In the solid layer, precipitation particles are heterogeneous and composed of a mixture of air and ice water. The refractive index of these mixtures is calculated by the ''matrix inclusion'' method proposed by Klaassen (1988) valid only for spherical particles. Let us suppose that a particle is composed of an element matrix containing inclusions of another element. The complex refractive index of the mixture can be written as follows:

$$m^2 = \frac{1 - f_{\text{inc}}}{1 - (1 - \beta)f_{\text{inc}}}m_{\text{mat}}^2 + \frac{\beta f_{\text{inc}}}{1 - (1 - \beta)f_{\text{inc}}}m_{\text{inc}}^2, \quad (13)$$

with

$$\beta = \frac{2m_{\text{mat}}^2}{m_{\text{inc}}^2 - m_{\text{mat}}^2}\left[\frac{m_{\text{inc}}^2}{m_{\text{inc}}^2 - m_{\text{mat}}^2}\log\left(\frac{m_{\text{inc}}^2}{m_{\text{mat}}^2}\right) - 1\right], \quad (14)$$

where $m^2$ is the complex refractive index of a matrix containing inclusions, the indices ''mat'' and ''inc'' stand for ''matrix'' and ''inclusion,'' respectively, and $f$ is the volume fraction of total particle volume.

In the solid layer, ice precipitation particles are formed of matrices of ice containing air inclusions. The refractive index can be derived from Eq. (13), with the volume fraction of air inclusions expressed as

$$f_{\text{mat}}(h) = f_s = \left(\frac{\rho_{s,\min}}{\rho_{s,\max}}\right)^{1-e} \text{ and}$$

$$f_{\text{inc}} = f_{\text{air}} = 1 - f_s, \quad (15)$$

with $\rho_{s,\min}$, $\rho_{s,\max}$, and $e$ as previously defined. It is considered a reasonable assumption that the value of $f_{\text{mat}}$ and consequently of $m^2$ and $\beta$ do not vary with altitude.

In the melting layer, precipitation particles are composed of liquid water with snow inclusions, which them-

selves are considered as mixtures of pure ice and air inclusions. The Klaassen concept is applied according to a two-step process. First, the equivalent complex refractive index of ice water (snow)—that is, a matrix of pure ice with air inclusions—is calculated with Eq. (13). Second, snow particles are used to represent the inclusions in a liquid water matrix. The equivalent complex refractive index of any particle can thus be calculated using

$$f_{\text{mat}}(h) = f_l(h) = \frac{f_m(h)}{f_m(h) + \left[\frac{\rho_l}{\rho(h)}\right][1 - f_m(h)]} \quad \text{and}$$

$$f_{\text{inc}}(h) = f_s(h) = 1 - f_l(h). \tag{16}$$

*e. Vertical profile of the drop size distribution*

The vertical variations in parameter $\Lambda$ are assumed linear and defined by a slope expressed in terms of $\text{m}^{-1}$ $\text{m}^{-1}$; they are chosen such that the resulting VPR is consistent with observed profiles representative of meteorological conditions. The value at ground level $\Lambda$ ($h = 0$) is estimated from the rainfall rate $R$ (mm $\text{h}^{-1}$) according to the following relationship (Marshall and Palmer 1948):

$$\Lambda(h = 0) = 4100R^{-0.21}. \tag{17}$$

*f. VIL radar measurement*

The reflectivity radar measurement can be written in the following form:

$$\overline{Z}_e(x, \theta_0, A) = \int_{h^-(\theta_0,A,x)}^{h^+(\theta_0,A,x)} g^2(\theta_0, h) Z_e(h)\, dh, \tag{18}$$

where $\overline{Z}_e$, the equivalent radar-measured reflectivity factor, depends on the distance $x$ between the radar and measurement point, elevation angle $A$, and radar beam width $\theta_0$; $h^-$ and $h^+$ denote the lower and upper limits of the radar beam, respectively, and depend on radar operating conditions $A$, $\theta_0$, and $x$; $g$ represents the partial integral of the radar beam power distribution at altitude $h$; and $Z$ denotes the reflectivity.

The VIL radar measurement is usually deduced from discrete radar observations between the ground level and the radar echo top, resulting in the following expression:

$$\text{VIL}^*(x, \theta_0) = (h_n^+ - h_1^-) \sum_{i=1}^{i=n} c\overline{Z}_e^{\,d}(x, \theta_0, A_i), \tag{19}$$

where VIL* is the VIL (kg $\text{m}^{-2}$) radar measurement; $n$ the number of radar bins along a vertical; $A_i$ the elevation angle for radar bin number $i$; $h_n^+$ and $h_1^-$, respectively, the top altitude of the highest radar bin and the bottom altitude of the lowest bin; and $c$ and $d$ the parameters of the adopted $Z_e$–$M$ relationship.

*g. Summary of model operations*

This section provides a summary of the construction of vertical profiles of both water content and reflectivities. Two hypothetical vertical profiles of DSD are provided; each is representative of a distinct meteorological situation: stratiform (denoted SVP) and convective (denoted CVP). Regarding SVP, the vertical profile of $\Lambda$ allows to retrieve a VPR typical of a stratiform situation, as described by Fabry and Zawadski (1995). Set at a constant value below the top of the melting layer, $\Lambda$ increases to reach a decrease in $Z$ of about 7 dB$Z$ $\text{km}^{-1}$ in the solid layer. The echo top is determined by the reflectivity, whose value is equal to the minimum detectable reflectivity (which corresponds to a radar constant $C = -62$ dBm and a minimum detectable signal equal to $-110$ dBm). For CVP, the vertical variations of $\Lambda$ are consistent with the mean VPR derived from the convective rainfall events observed during Hydromet International Radar Experiment (HIRE) (see section 6). The term $\Lambda$ rises in order to attain a decrease of 0.66 dB$Z$ $\text{km}^{-1}$ for $Z_e$ in the liquid, melting, and solid layers.

The first stage of operations consists of defining both the rainfall rate at ground level $R_0$, the surface temperature $T_0$, and the type of rainfall event: stratiform versus convective. This stage allows characterizing the DSD at ground level, with $N_0$ and $\Lambda$ being adapted to the type and intensity of rainfall event. The rate of change of $\Lambda$ is chosen, according to the type of rainfall event. The temperature decrease with altitude is assumed to follow the saturated adiabat, which yields the 0°C isotherm. The solid layer is characterized by two parameters: the increase rate in DSD parameter $\Lambda$, and the density factor (which is defined according to the type of rainfall event). The melting layer thickness is estimated by means of the empirical relationship proposed by Fabry and Zawadski (1995) where $Z_e$ is expressed in $\text{mm}^6$ $\text{m}^{-3}$:

$$h_{\text{iso0}} - h_{\min} = 140Z_e^{0.17}. \tag{20}$$

The echo top $h_t$ (m) is related to the rainfall rate $R$ (mm $\text{h}^{-1}$) by virtue of the observation provided by Adler and Mack (1984):

$$h_t = 2690R^{0.41}. \tag{21}$$

The profiles of $\Lambda$, reflectivity, mass density, and dielectric constant are all shown in Fig. 2. Table 1 lists the parameter values serving to define the two theoretical vertical profiles of DSD and indicates the corresponding true VIL values: $\text{VIL}_{\text{SVP}} = 0.59$ kg $\text{m}^{-2}$ and $\text{VIL}_{\text{CVP}} = 6.96$ kg $\text{m}^{-2}$.

## 4. Assessment of the sources of error in VIL radar measurement

This section is intended to quantify the magnitude of errors occurring in VIL radar measurement. The reference is composed of vertical profiles of DSD of

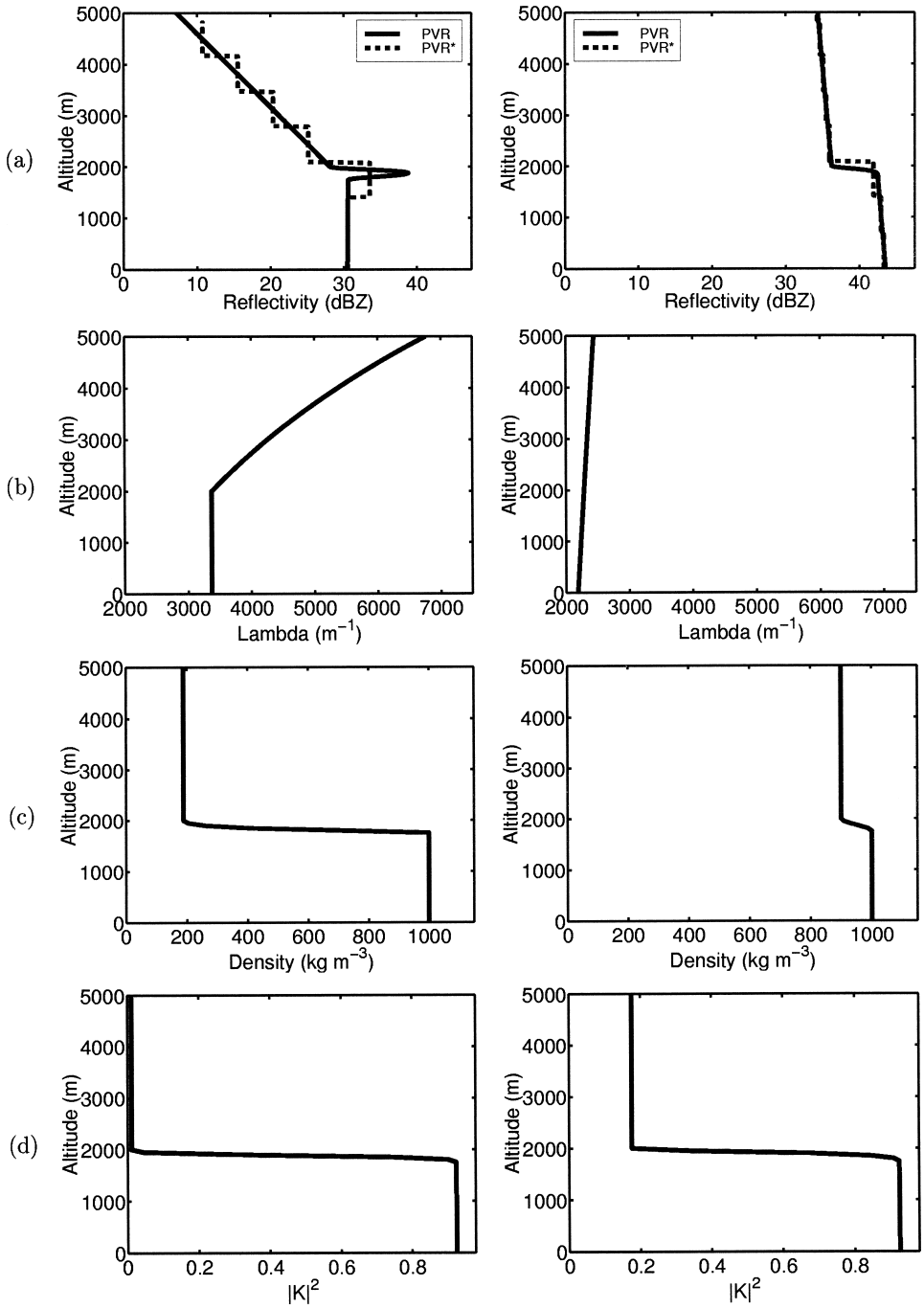


FIG. 2. Vertical profiles for the (left) reference stratiform profile, $e = 0.7$, and the (right) reference convective profile, $e = 1.0$, of (a) reflectivity, (b) second DSD parameter $\Lambda$, (c) mass density, and (d) dielectric factor.

precipitation particles, which provide the true VIL [Eq. (3)] while serving to calculate the reference VPR used to simulate the VIL radar estimation, in accordance with the model described in section 2 (see Fig. 1). This error analysis is based on the two hypothetical vertical profiles of DSD introduced in the previous section, which are representative of stratiform and convective meteorological situations, respectively.

The $Z_e$–$M$ relationship (Amburn and Wolf 1997), classically used to estimate the VIL, is established by combining the integral definitions of both reflectivity

TABLE 1. Values of the parameters defining the two reference vertical profiles of DSD and values of the resulting VIL.

| | Convective theoretical profile (CVP) | Stratiform theoretical profile (SVP) |
|---|---|---|
| Rainfall rate (mm $h^{-1}$): $R_0$ | 20 | 3 |
| Density factor: $e$ | 1 | 0.7 |
| Second parameter of DSD: $\Lambda$ | Rising in order to attain a decrease of 7 dBZ $km^{-1}$ for $Z_e$ in the solid layer | Rising in order to attain a decrease of 0.66 dBZ $km^{-1}$ for $Z_e$ |
| VIL (kg $m^{-2}$) | 6.96 | 0.59 |

and water content and in assuming the Rayleigh approximation with $N_0 = 8 \times 10^6$ $m^{-4}$:

$$M = 3.44 \times 10^{-6} Z_e^{4/7}. \quad (22)$$

In this expression, $M$ is the water content expressed in kg $m^{-3}$ and $Z_e$ is expressed in $mm^6$ $m^{-3}$.

For this error analysis, the radar displays the following features: a 5-cm wavelength, a 3-dB beamwidth $\theta_0 = 1.3°$, a lowest elevation angle $A_1 = 0.65°$, and an elevation angle increment of 1.3°, which means that adjacent 3-dB radar beams are contiguous. Various measurement distances will be tested, ranging from 30 to 100 km. It is assumed that the number of elevation angles is large enough to allow for a complete sampling of the vertical profile. If radar beams were not contiguous, an interpolation procedure would be needed to fill in the vertical profile of reflectivity. This additional source of error in the VIL measurement is not addressed in this study. The measurement error is quantified by the relative error (denoted RE and expressed in percent) between the true VIL and the VIL value measured by radar (VIL*), as follows:

$$\text{RE} = \frac{\text{VIL} - \text{VIL}^*}{\text{VIL}} \times 100. \quad (23)$$

The results of this error analysis have been summarized in Fig. 3 and give rise to the following general comments. In the convective situation (CVP), VIL is likely to be significantly underestimated (by about 40%). This underestimation can be explained (Fig. 4) by the fact that the classical $Z_e$–$M$ relationship is not well-suited to the ice phase of water particles. In the stratiform situation, no significant bias is found in the VIL measurement and measurement error varies over the interval [−10%, +10%] depending on conditions. This lack of bias can be explained by the fact that the overestimation due to the bright band compensates for the underestimation occurring in the solid phase. The following sections will discuss the influence of radar operating conditions and of meteorological condition on VIL estimation accuracy.

### *a. Influence of radar operating conditions*

The two radar parameters tested are beamwidth and distance to the radar. Three radar beamwidths have been considered herein (1.0°, 1.3°, and 1.6°) along with various distances. In all cases, it is assumed that the 3-dB beamwidths are contiguous. Figure 3a illustrates the evolution in relative error versus distance for the two reference vertical profiles of DSD. It appears that beamwidth does not significantly influence VIL error measurement regardless of the profile under consideration. The level of underestimation remains unchanged for the CVP. The measurement error stays within the interval [−10%, +10%] for the reference SVP. The random fluctuations of measurement error in the latter case are due to variations in distance to the intersection between radar beam and bright band.

### *b. Influence of meteorological conditions*

The VIL measurement error may depend on meteorological conditions, which are represented by the characteristics of the vertical profile of DSD of precipitation particles. The sensitivity analysis of VIL error entails the following parameters: (i) the 0°C altitude, which controls the water phase change; and (ii) the density factor and DSD profile for raindrops. All of these parameters exert an influence on the $Z_e$–$M$ relationship, which serves to derive the snow, graupel, and rainwater content from equivalent radar reflectivity factor.

The influence of the 0°C altitude, as illustrated in Fig. 3c, depends on the type of rainfall event. For the convective event (CVS), VIL measurement accuracy falls when the 0°C altitude decreases regardless of distance (from −30% to −50%). This finding is due to the growing portion of the profile being ascribed to the solid layer, which displays different backscattering characteristics. The stratiform profile is much less affected by changes in the 0°C altitude, although a drop in measurement accuracy can be detected for low values of the 0°C isotherm.

The density factor is related to the mass density of ice water particles. The magnitude of the brightband peak depends on the value of the density factor above the melting layer. As indicated in Table 2, a high $e$ value corresponds to a weak brightband peak while a low $e$ value corresponds to a high brightband peak. The stratiform situation (SVP) corresponds to an $e$ value ranging from about 0.6 to 0.8. A systematic overestimation of the actual VIL is associated with very low values of the density factor (see Fig. 3b); in this case, the overestimation of VIL due to the bright band does not compensate for the underestimation due to an unsuitable $Z_e$–$M$ relationship for ice particles. As $e$ increases, the bias

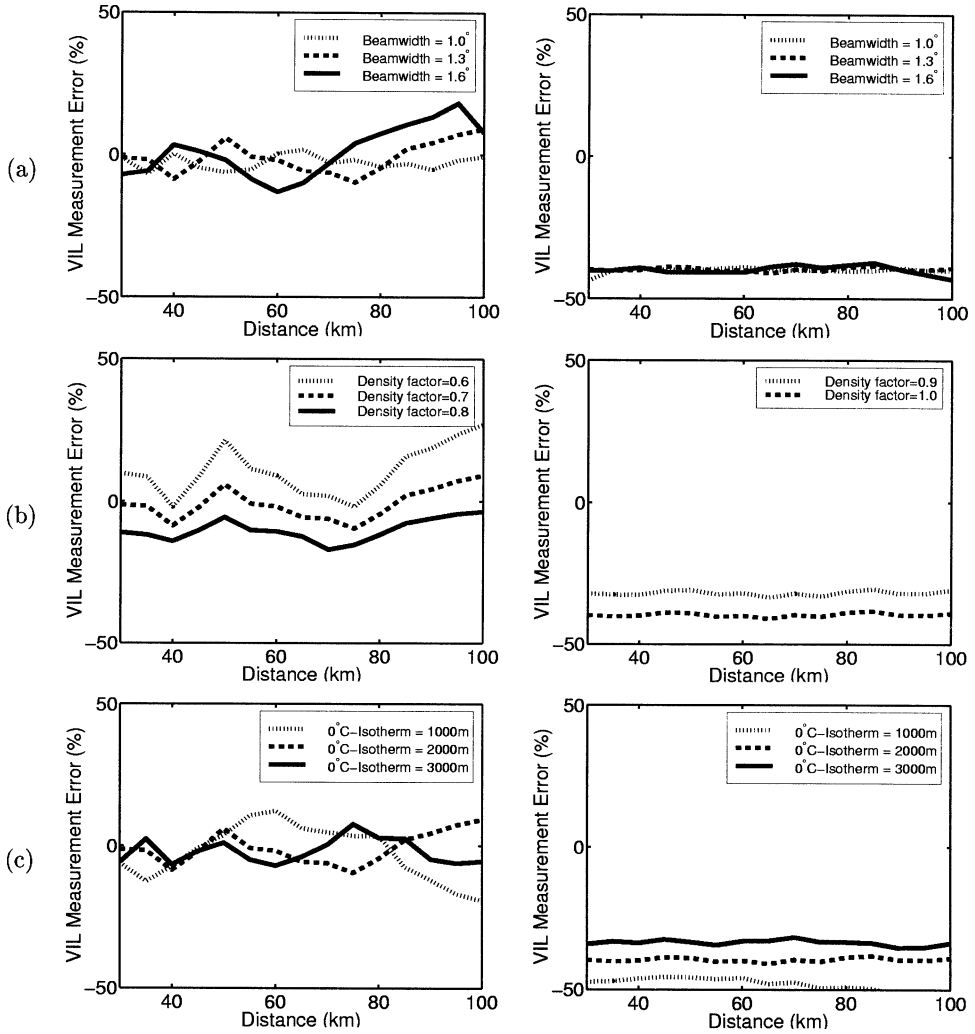


FIG. 3. Assessment of the sources of error in VIL radar measurement for reference profiles. VIL error measurement vs distance for (left) the reference stratiform profile and (right) for the reference convective profile. (a) Influence of beamwidth, (b) influence of density factor, and (c) influence of 0°C isotherm altitude.

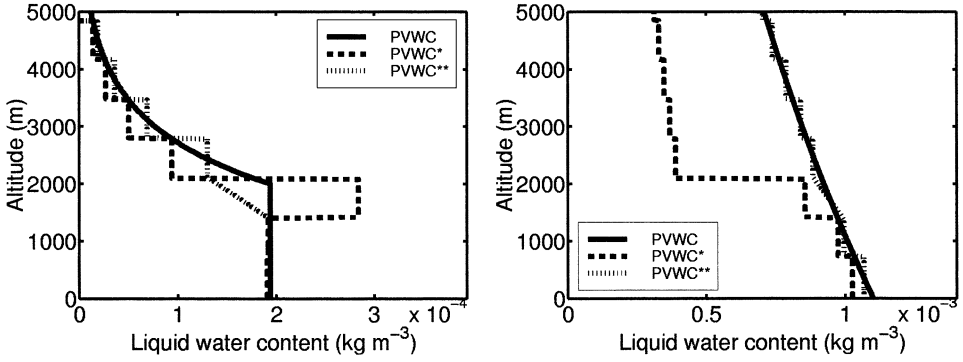


FIG. 4. Vertical profile of water content at a distance of 30 km for the (left) reference stratiform and (right) convective profile. PVWC corresponds to the actual profile, PVWC* represents the profile obtained by the classical method, whereas PVWC** corresponds to the profile obtained by the alternative method (presented in section 5).

TABLE 2. Values of peak of reflectivity vs density factor for the reference stratiform profile.

| Density factor $e$ | Mass density $\rho_s$ (kg m$^{-3}$) | Peak of reflectivity (dBZ) |
|---|---|---|
| 0.6 | 113 | +13 |
| 0.7 | 190 | +10 |
| 0.8 | 319 | +7 |
| 0.9 | 535 | +4 |

becomes negligible and VIL stands between −10% and 10%. For the convective situation, underestimation increases with the value of $e$, that is, as graupels become closer to pure ice.

In conclusion, the most influential parameters with respect to VIL measurement accuracy are: the characteristics of the vertical profile of DSD and the density factor. Both are associated with the contrast existing between the backscattering characteristics of solid water particles and liquid raindrops. This finding confirms that the use of a single $Z_e$–$M$ relationship for all the vertical radar bins does not appear adapted to an accurate VIL radar measurement. The next section presents a simple method for helping improve this accuracy.

## 5. A simple method for improving VIL measurement

The sensitivity analysis conducted in the previous section has demonstrated that the classical method for estimating VIL results in (i) an underestimation due to the use of a $Z_e$–$M$ relationship ill-adapted to ice water particles in convective situations, and (ii) a smaller measurement error for stratiform situations, due to the offset of two sources of error. In order to reduce VIL measurement error, it is proposed herein to test the following simple alternative method, which consists of the following.

- Using two distinct $Z_e$–$M$ relationships on both sides of the 0°C isotherm, adapted to raindrops in the lower part of the profile and to snow (for the stratiform situation) or ice (convective situation) in the upper part. The $Z_e$–$M$ relationship adapted to ice water is computed with the same technique, but by taking the mass density related to $e$ into account; moreover, this relationship is uniformly applied within the solid layer.
- Replacing the reflectivity factor of the radar bins intersecting the melting layer by a linear interpolation of reflectivity factors on both sides separating this area.

The practical application of this alternative method requires, in all cases, estimating the values of both the 0°C altitude (iso0) and the density factor ($e$) in the solid layer, as the values of these two parameters are never precisely known. Equation (20) is used to determine the melting layer thickness.

An initial evaluation of the alternative method has been conducted under perfect conditions. This evaluation is based on the two reference profiles (CVP and SVP). We have assumed that: the method's application conditions are not subjected to any source of error and both the density factor and 0°C-isotherm altitude are precisely known. This assumption, of course, does not represent a real-world situation. Figure 5a displays the results obtained with the alternative and classical methods; these results confirm the potential interest of the alternative method, which reduces overestimation due to the bright band while reducing underestimation due to the unsuitable classical $Z_e$–$M$ relationship. In order to take the uncertainty on the 0°C-isotherm altitude and on the density factor into account, the previous test has been performed again under the following assumptions.

- The estimation of the 0°C isotherm is affected by an error on the 0°C altitude distributed according to an unbiased Gaussian law, with a standard deviation error of 100 or 200 m; and
- the $Z_e$–$M$ relationship for ice particles corresponds to an error of the density factor, which follows an unbiased Gaussian law with a standard deviation of 0.1 or 0.2.

The results obtained are presented in Figs. 5b–d, which indicate that errors introduced in estimating the freezing level or density factor are not detrimental to the alternative method, which remains more efficient than the classical method. Nevertheless, this conclusion only applies to the reference vertical profiles of DSD used in the sensitivity analysis. The next section will focus on a validation procedure that proves to be more consistent with real-world VIL measurements.

## 6. An evaluation of VIL measurement from actual radar data

### *a. Presentation of the case study*

A real-world validation would require comparison between VIL radar measurement and direct measurement, but such a comparison remains entirely impossible. Despite this difficulty, an evaluation of VIL radar measurement, based on actual vertical profiles of reflectivity, has been conducted. The dataset was taken from the HIRE experiment (Uijlhenhoet et al. 1999), which took place in Marseille from September to November 1998. During this period, 12 various types of rainfall events (stratiform, convective, autumn storms, etc.) all characteristic of this region occurred. These events were either partially or totally recorded by various sensors, including an X-band vertically pointing radar operated by the University of Bristol. This radar samples the atmospheric structure with both a very short temporal period (4 s) and a very detailed spatial resolution (7.5 m). The validation of VIL measurement is performed in two stages: definition of the reference VILs, and ap-

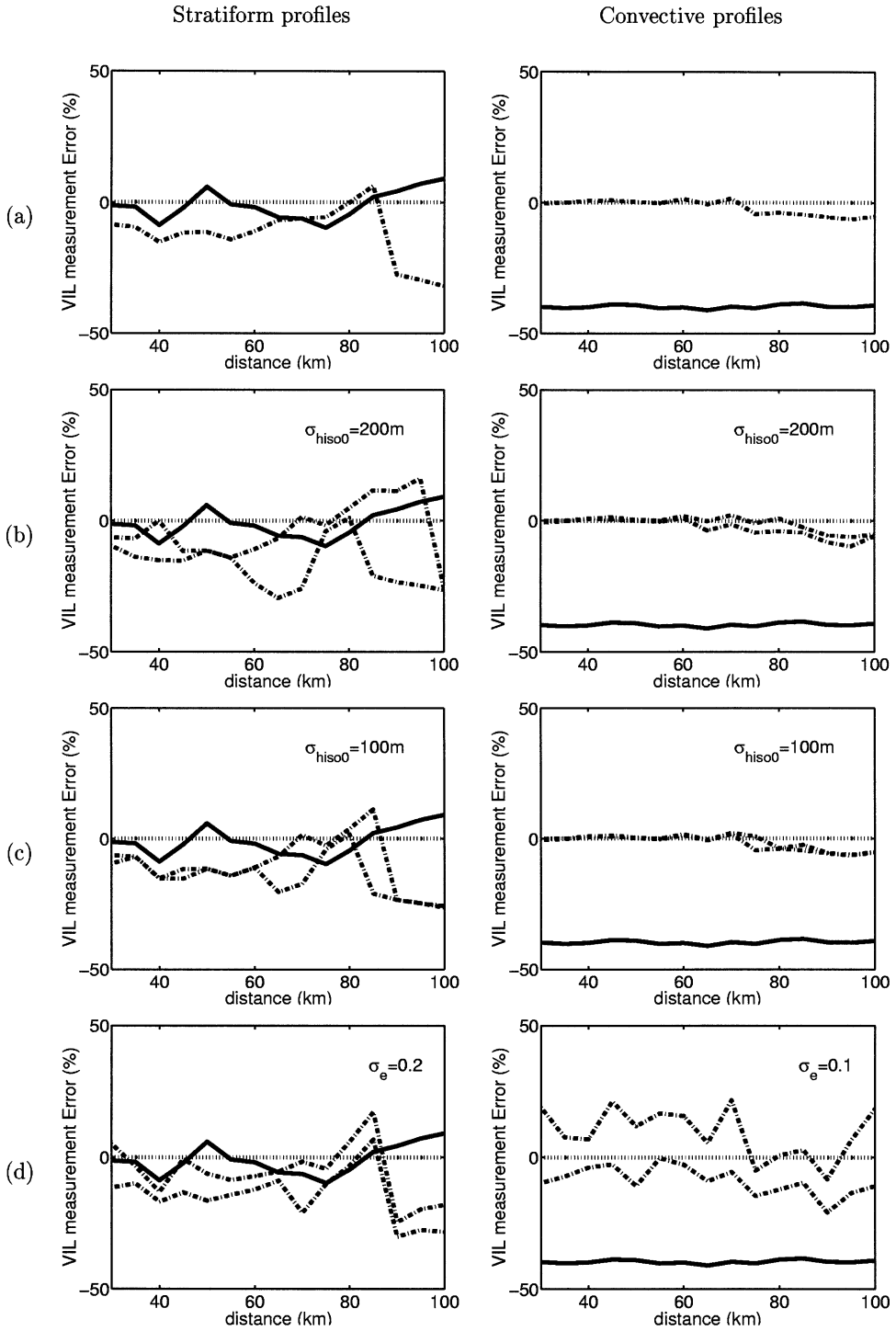


FIG. 5. VIL measurement error with both the classical and alternative methods for the (left) reference stratiform and (right) convective profiles: (a) if the density factor and 0°C-isotherm altitude are precisely known, (b) considering a 200-m bias error on the 0°C-isotherm altitude, (c) considering a 100-m bias error on the 0°C-isotherm altitude, and (d) considering a 0.2 (for the stratiform profile) or 0.1 (convective profile) bias error on the density factor. Solid lines correspond to the classical method and dashed lines to the alternative method. On graphs (b), (c), and (d), the two-dashed lines represent the bounds of the 95% confidence interval.

TABLE 3. Mean RE and std dev on VIL measurement errors obtained with the classical and alternative methods for actual convective and stratiform profiles.

| | Convective profiles | | | Stratiform profiles | | |
|---|---|---|---|---|---|---|
| | 30 km | 60 km | 90 km | 30 km | 60 km | 90 km |
| Mean: $\mu_{RE}$ (%) | | | | | | |
| Classical method | −26.18 | −31.84 | −33.61 | −28.48 | −36.28 | −42.40 |
| Alternative method With $\sigma_{hiso0}$ = 100 m and $\sigma_e$ = 0.1 | −13.23 | −20.43 | −21.04 | −5.59 | −19.73 | −29.66 |
| Alternative method With $\sigma_{hiso0}$ = 200 m and $\sigma_e$ = 0.2 | −14.76 | −21.40 | −21.70 | −6.16 | −20.66 | −29.33 |
| Standard deviation: $\sigma_{RE}$ (%) | | | | | | |
| Classical method | 14.50 | 15.91 | 18.59 | 9.15 | 12.47 | 13.23 |
| Alternative method With $\sigma_{hiso0}$ = 100 m and $\sigma_e$ = 0.1 | 14.03 | 17.30 | 19.53 | 10.33 | 18.27 | 19.44 |
| Alternative method With $\sigma_{hiso0}$ = 200 m and $\sigma_e$ = 0.2 | 14.31 | 17.37 | 19.16 | 12.73 | 18.61 | 20.82 |

plication of the VIL measurement methods. A total of 1080 observed vertical profiles of reflectivity are used for this purpose, 515 of which are classified as stratiform (SVP) by virtue of displaying a visible bright band that allows visually determining the 0°C altitude with good accuracy. The 565 remaining observed profiles have been designated convective (CVP). The 0°C altitude has been estimated from information provided by stratiform profiles recorded over a narrow time interval.

Defining the reference VIL requires transforming the VPRs recorded by the vertically pointing radar into vertical profiles of DSD. This retrieval procedure is based on the theoretical model presented in section 2, which has been slightly modified in order to adapt to actual observations—that is, (i) in the liquid phase, the value of $\Lambda$ is directly deduced from observed reflectivities; and (ii) the density factor is estimated from the magnitude of the brightband peak, according to results of the theoretical model (see Table 2). Moreover, this procedure allows the determinination of vertical profiles of water content that are both realistic and fully consistent with the observed VPRs. The reference VILs are directly derived from these profiles; nevertheless, it must be kept in mind that these vertical profiles of water content are not true profiles, since the true profiles remain unknown.

### *b. Evaluation of VIL measurement methods*

The method is evaluated as follows. The volume scan radar data are derived from vertically pointing radar data. The 3-dB beamwidth is $\theta_0 = 1.3°$, the incremental elevation angle between successive beam widths is 1.3°. Three distances 30, 60, and 90 km are considered in order to cover the hydrological range of application of a weather radar. The VIL is estimated from these VPRs according to the two following methods:

1) the classical VIL measurement method [Eq. (22)], which corresponds to liquid water, is applied; and
2) the alternative VIL measurement method requires knowledge of both the 0°C-isotherm altitude and the density factor. It is assumed that (i) the error on the 0°C altitude is distributed according to an unbiased Gaussian law with a standard deviation error of 200 m, and (ii) the error of the density factor follows an unbiased Gaussian law with a standard deviation of 0.2.

The two VIL values obtained with the alternative and classical methods are then compared to the reference VIL value with the evaluation criterion being the mean relative error. The obtained results are displayed in Table 3 and plotted in Fig. 6 and Fig. 7, which display the histograms of the relative error for the set of 515 stratiform and 565 convective profiles at distances of 30, 60, and 90 km. Figure 6 shows that the classical method leads to a significant underestimate of the VIL, whatever the distance. The alternative method reduces this bias and provides better VIL estimates. Nevertheless, results obtained with the alternative method are not totally conclusive. The amplitude of the scattergram relative errors associated with the alternative method is equal or even larger than the one associated with classical method. These conclusions remain valid for stratiform profiles (Fig. 7).

In summary, an evaluation of the VIL radar measurement, based on a set of vertical profiles of reflectivity recorded by a high-resolution vertically pointing radar, has been performed. This evaluation confirms that the classical VIL measurement method is likely to lead to an underestimation of the true VIL; moreover, it indicates that improvement can be obtained by applying a simple alternative method, which distinguishes the liquid and solid water particles. This alternative method requires information on both the 0°C-isotherm altitude and the density factor. If these two parameters can be estimated with reasonable confidence, the method proves to be quite efficient.

## 7. Conclusions

This study has been intended to assess the accuracy of VIL estimation, which constitutes a product of weath-

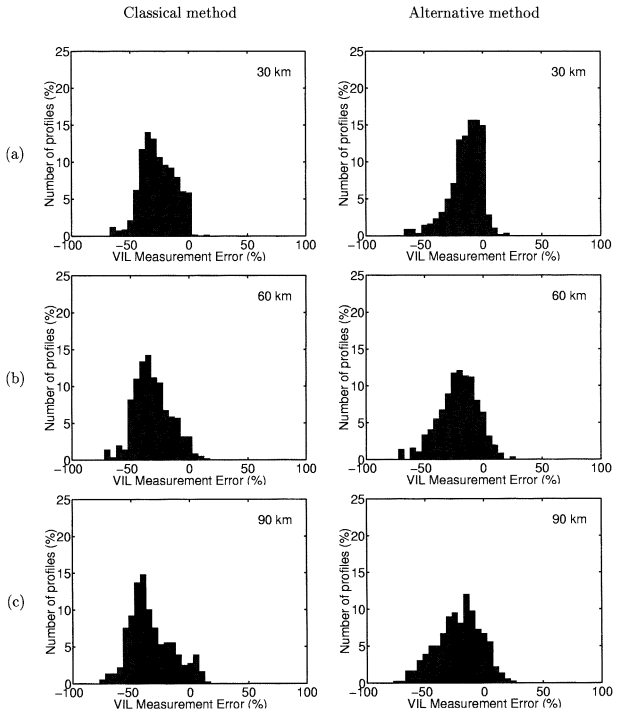


FIG. 6. VIL measurement error for convective profiles with the radar at (a) 30, (b) 60, and (c) 90 km. (left) VIL measurement error obtained using the classical method, and (right) error obtained using the alternative method. The error on the 0°C-isotherm altitude, and the density factor are distributed according to an unbiased Gaussian law, with an std dev of 200 m and 0.2, respectively.

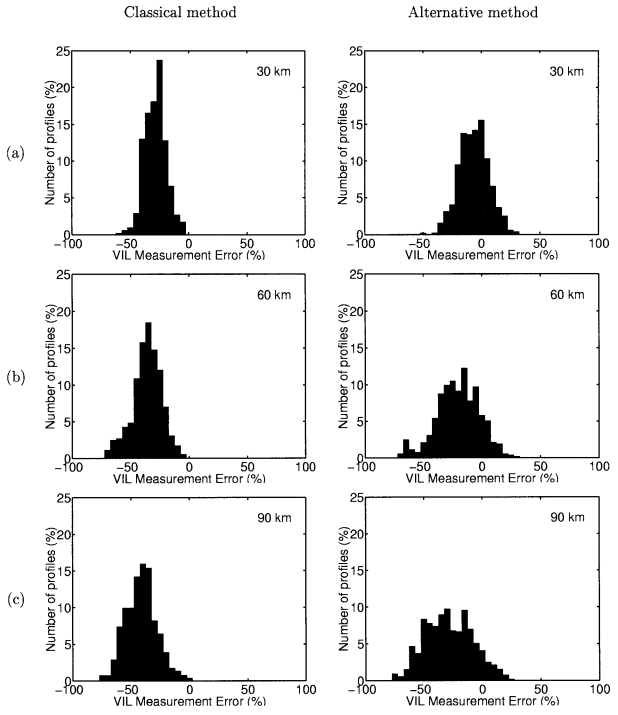


FIG. 7. VIL measurement for stratiform profiles with the radar at (a) 30, (b) 60, and (c) 90 km. (left) VIL measurement error obtained using the classical method, and (right) error obtained using the alternative method. The error on the 0°C-isotherm altitude and the density factor are distributed according to an unbiased Gaussian law, with an std dev of 200 m and 0.2, respectively.

er radars performing voluminal scanning. This evaluation has been conducted by means of simulation, due to the absence of reference measurements. The reference VIL has been derived from a reference vertical profile of DSD, defined by including the various states of water particles: liquid, solid, and melting. Furthermore, a model has been developed in order to (i) simulate the vertical profile of reflectivity corresponding to the vertical profile of DSD, and (ii) calculate the VIL that would be obtained by using the classical method based on a $Z_e$–$M$ relationship adapted to liquid precipitation water. The VIL measurement error, for a given vertical profile of DSD (i.e., for a given meteorological situation), is obtained by comparing the reference VIL to the VIL measurement simulated by the model. During an initial stage, two reference profiles representing two distinct meteorological situations were used: the first represents stratiform rainfall events, while the second represents convective rainfall events. A sensitivity analysis of both the meteorological conditions and radar operating conditions reveals that VIL measurement errors related to meteorological conditions are significant. For a convective situation, the level of underestimation ranges over the interval [−20%, −40%], whereas in stratiform situations the measurement error is more variable (over the interval [−10%, +10%]) and lends the impression of being smaller. This outcome is due to the compensation taking place between the brightband effect and underestimation occurring in the solid phase.

An alternative method has been proposed to limit measurement errors; this method consists of removing the radar bins corresponding to the 0°C isotherm and adapting the $Z_e$–$M$ relationship to the type of water particles: liquid or solid. The method has been applied to the two adopted profiles, and its sensitivity to the required parameters (i.e., 0°C-isotherm altitude and density factor) has been tested. Improvements to VIL measurement are indeed possible thanks to this method, despite approximate knowledge of the parameters. Both the classical and alternative VIL measurement methods were tested and compared on a dataset that combines VPRs observed by a vertically pointing radar. This test, which more closely resembles actual measurement conditions than the reference VPRs, indicates that as 0°C-isotherm altitude increases and the density of ice particles becomes precisely known, the alternative method reduces measurement error to a greater extent.

The simplicity of the alternative VIL measurement method makes it appealing for practical use in real-time VIL measurement algorithms. Before its implementation, this method should undergo testing on a larger number of actual situations, by means of comparing the estimations provided by both methods. Moreover, it would be worthwhile to assess the interest of polari-

zation techniques in improving determination of the 0°C altitude and better distinguishing hydrometeors, in addition perhaps to estimating the density factor.

*Acknowledgments.* This work was supported by the PATOM (Program ''ATmosphere and Ocean at Multiscale'') and coordinated by the French organisations CNRS/INSU. The authors would like to thank the two anonymous reviewers for their comments helpful in improving the manuscript.

## REFERENCES

Adler, R. F., and R. A. Mack, 1984: Thunderstorm cloud height-rainfall rate relations for use with satellite rainfall estimation techniques. *J. Climate Appl. Meteor.,* **23,** 280–296.

Amburn, S. A., and P. W. Wolf, 1997: VIL density as a hail indicator. *Wea. Forecasting,* **12,** 473–478.

Andrieu, H., M. N. French, V. Thauvin, and W. F. Krajewski, 1996: Adaptation and application of a quantitative rainfall forecasting model in a mountainous region. *J. Hydrol.,* **184,** 234–259.

Atlas, D., R. Srivastava, and R. Sekhon, 1973: Doppler radar characteristics of precipitation at vertical incidence. *Rev. Geophys. Space Phys.,* **11,** 1–35.

Battan, L. J., 1973: *Radar Observations of the Atmosphere*. University of Chicago Press, 324 pp.

Billet, J., M. DeLisi, and B. G. Smith, 1997: Use of regression techniques to predict hail size and the probability of large hail. *Wea. Forecasting,* **12,** 154–164.

Borga, M., E. M. Anagnostou, and W. F. Krajewski, 1997: A simulation approach for validation of a brightband correction method. *J. Appl. Meteor.,* **36,** 1504–1518.

Collier, C. G., Ed., 2001: COST 75: Advanced weather radar systems 1993–1997 final report. Office of Publication of European Communities, Brussels, Germany.

Delrieu, G., J. D. Creutin, and I. Saint-André, 1991: Mean K–R relationships: Practical results for typical weather radar wavelengths. *J. Atmos. Oceanic Technol.,* **8,** 467–476.

Dolcine, L., H. Andrieu, M. N. French, and J. D. Creutin, 2000: Implementation considerations of a conceptual precipitation model. *J. Geophys. Res.,* **105,** 2291–2297.

Ducrocq, V., J. P. Lafore, J. L. Redelsperger, and F. Orain, 2000: Initialization of a fine scale model for convective system prediction: A case study. *Quart. J. Roy. Meteor. Soc.,* **126,** 3041–3066.

Edwards, R., and R. L. Thompson, 1998: Nationwide comparisons of hail size with WSR-88D vertically integrated liquid water and derived thermodynamics sounding data. *Wea. Forecasting,* **13,** 277–285.

Fabry, F., and I. Zawadzki, 1995: Long-term radar observations of the melting layer of precipitation and their interpretation. *J. Atmos. Sci.,* **52,** 838–850.

French, M. N., and W. F. Krajewski, 1994: A model for real-time quantitative rainfall forecasting using remote sensing. Part 1: Formulation. *Water Resour. Res.,* **30,** 1075–1083.

——, H. Andrieu, and W. F. Krajewski, 1995: Uncertainty in vertically integrated liquid water content due to radar reflectivity observation error. *J. Atmos. Oceanic Technol.,* **12,** 404–409.

Georgakakos, K. P., and R. L. Bras, 1984: A hydrologically useful station precipitation model. Part 1: Formulation. *Water Resour. Res.,* **20,** 1585–1596.

Hardaker, P. J., A. R. Holt, and C. G. Collier, 1995: A melting-layer model and its use in correcting for the bright band in single-polarization radar echoes. *Quart. J. Roy. Meteor. Soc.,* **121,** 495–525.

Kitzmiller, D. H., W. E. McGovern, and R. F. Saffle, 1995: The WSR-88D severe weather potential algorithm. *Wea. Forecasting,* **10,** 141–159.

Klaassen, W., 1988: Radar observations and simulation of the melting layer of precipitation. *J. Atmos. Sci.,* **45,** 3741–3752.

Klazura, G. E., and D. A. Imy, 1993: A description of the initial set of analysis products available from the NEXRAD WSR-88D system. *Bull. Amer. Meteor. Soc.,* **74,** 1293–1311.

Lee, T. H., and K. P. Georgakakos, 1990: A two-dimensional stochastic-dynamical quantitative precipitation forecasting model. *J. Geophys. Res.,* **95,** 2113–2126.

——, and ——, 1996: Operational rainfall prediction on mesoscales for hydrologic applications. *Water Resour. Res.,* **32,** 987–1003.

MacKeen, P., H. Brooks, and K. Elmore, 1997: The merit of severe and non-severe thunderstorm parameters in forecasts of thunderstorm longevity. Preprints, *28th Conf. on Radar Meteorology*, Austin, TX, Amer. Meteor. Soc., 424–425.

Marshall, J. S., and W. M. K. Palmer, 1948: The distribution of raindrops with size. *J. Meteor.,* **5,** 165–166.

Nakakita, E., S. Ikebuchi, T. Nakamura, M. Kanmuri, M. Okuda, A. Yamaji, and T. Takasao, 1996: Short-term rainfall prediction method using a volume scanning radar and grid point value data from numerical weather prediction. *J. Geophys. Res.,* **101,** 26 182–26 197.

Pruppacher, H. R., and J. D. Klett, 1978: *Microphysics of Clouds and Precipitation.* D. Reidel, 714 pp.

Rogers, R. R., and M. K. Yau, 1989: *A Short Course in Cloud Physics.* Pergamon Press, 293 pp.

Russchenberg, H. W. J., 1992: Ground-based remote sensing of precipitation using a multi-polarized FM-CW Doppler radar. Ph.D. thesis, Delft University, 206 pp.

Sempere Torres, D., J. M. Porrà, and J.-D. Creutin, 1994: A general formulation for raindrop size distribution. *J. Appl. Meteor.,* **33,** 1494–1502.

Seo, D. J., and J. A. Smith, 1992: Radar-based short-term rainfall prediction. *J. Hydrol.,* **131,** 341–367.

Shafer, M. A., D. R. MacGorman, and F. H. Carr, 2000: Cloud-to-ground lightning throughout the lifetime of a severe storm system in Oklahoma. *Mon. Wea. Rev.,* **128,** 1798–1816.

Sugimoto, S., E. Nakakita, and S. Ikebuchi, 2000: A stochastic approach to short-term rainfall prediction using a physically-based conceptual rainfall model. *J. Hydrol.,* **242,** 137–155.

Szyrmer, W., and I. Zawadzki, 1999: Modeling of the melting layer. Part I: Dynamics and microphysics. *J. Atmos. Sci.,* **56,** 3573–3592.

Thielen, J., B. Boudevillain, and H. Andrieu, 2000: A radar data based short-term rainfall prediction model for urban areas—A simulation using meso-scale meteorological modelling. *J. Hydrol.,* **239,** 97–114.

Uijlenhoet, R., and Coauthors, 1999: Hydromet Integrated Radar Experiment (HIRE): Experimental setup and first results. Preprints, *29th Int. Conf. on Radar Meteorology*, Montreal, PQ, Canada, Amer. Meteor. Soc., 926–930.

Willis, T. W., and A. J. Heymsfield, 1989: Structure of the melting layer in mesoscale convective system stratiform precipitation. *J. Atmos. Sci.,* **46,** 2008–2025.